Upwind compact scheme with dispersion control for aerodynamic equations*

Ma Yanwen and Fu Dexun
马延文 傅德薰

Open Laboratory for Nonlinear Continuous Media Mechanics, Institute of Mechanics, Academy of Science, Beijing 100080

(Received 17 October 1990)
Chin. J. Comp. Phys. **8**(3), 287–294 (September 1991)

A compact upwind scheme with dispersion control is developed using a dissipation analogy of the dispersion term. The term is important in reducing the unphysical fluctuations in numerical solutions. The scheme depends on three free parameters that may be used to regulate the size of dissipation as well as the size and direction of dispersion. A coefficient to coordinate the dispersion is given. The scheme has high accuracy, the method is simple, and the amount of computation is small. It also has a good capability of capturing shock waves. Numerical experiments are carried out with two-dimensional shock wave reflections and the results are very satisfactory.

I. INTRODUCTION

Realistic flow fields are quite complex in general, consisting of shock waves, separated flows, eddy motion, as well as interferences between them. Because of limitations in computational techniques, it is an important question in aerodynamics to improve the accuracy of the numerical solution and the efficiency of the solution.

Higher-accuracy schemes produce more accurate numerical solutions and increase the computational efficiency by decreasing the number of grid points. In Ref. 1, the problem of a blunt object in supersonic viscous circular flow was treated by a nonconservative, compact scheme. In Ref. 2, the same problem was treated using a conservative, compact scheme. Compared with the usual high-accuracy schemes, these approaches have even better accuracies. Furthermore, the amount of computation is less and boundary conditions can be handled with ease. However, the disadvantage is that, near shock waves, the numerical solutions have nonphysical fluctuations.

To overcome the fluctuations, we construct here an upwind compact scheme with dispersion control. In this type of scheme, it is possible to regulate the size of dispersion and, hence, the accuracy. It is also possible to control the size and direction of the dispersion. By controlling the dissipation and dispersion, better discrimination is achieved in the numerical solution. The second section of this paper deals with the decomposition of one-dimensional aerodynamic equations and Jacobian coefficient matrices. The finite difference approximation of the model equation is given in Sec. III. We present there also the theory behind the compact scheme, the upwind compact scheme, and the upwind compact scheme with dispersion control. Section IV describes an upwind compact scheme with dispersion control for the one-dimensional Euler equation. A numerical experiment is carried out on a finite difference scheme arising from a two-dimensional shock-wave reflection problem.

II. 1-D EULER EQUATION AND DECOMPOSITION OF THE JACOBIAN MATRIX

For the convenience of subsequent discussion, we shall give here a brief introduction to the decomposition of the equation and the Jacobian coefficient matrix.

 0273-429X/92/041015-09$03.00

2.1 One-dimensional Euler equation

After converting to dimensionless units, the vector form of the equation may be written as

$$\frac{\partial U}{\partial t} + \frac{\partial f}{\partial x} = 0, \tag{1}$$

$$U=[\rho, \rho u, E]^{\mathrm{T}}, f=[\rho u, \rho u^2+p, u(E+p)]^{\mathrm{T}},$$

$$p=\frac{1}{\gamma M_\infty^2}\rho T, E=\rho(c_v T+\frac{u^2}{2}), \tag{2}$$

where ρ, u, and T are the dimensionless density, velocity, and temperature, respectively.

2.2 Decomposition of the Jacobian coefficient matrix

Let A be the Jacobian coefficient matrix

$$A=\frac{D(f)}{D(U)}.$$

It may be represented by a diagonal matrix

$$A=S^{-1}\Lambda S \quad, f=AU.$$

Here Λ is the diagonal matrix made of the characteristic values of A

$$\lambda_1=u \quad, \lambda_2=u-c, \quad \lambda_3=u+c. \tag{3}$$

We can use the decomposition of λ_k to decompose the matrix A and the flow vector f:

$$\lambda_k=\lambda_k^+ + \lambda_k^- \quad, \lambda_k^+ \geqslant 0, \ \lambda_k^- \leqslant 0, \tag{4}$$

$$A^\pm = S^{-1}\Lambda^\pm S \quad, f^\pm = A^\pm U.$$

Here $\Lambda^\pm$ are diagonal matrices made of $\lambda_k^\pm$. There are three different practical ways to carry out the decomposition:

(a) $$\lambda_k^\pm = \frac{1}{2}(\lambda_k \pm |\lambda_k|),$$

(b) $$\lambda_{1,2}^+ = u^+, \quad \lambda_3^+ = u^+ + c \quad, u^\pm = \frac{1}{2}(u \pm |u|),$$

$$\lambda_{1,3}^- = u^- \quad, \lambda_2^- = u^- - c,$$

(c) $$\lambda_k^+ = \lambda^+ \geqslant \max\{0, \lambda_k\},$$

$$\lambda_k^- = \lambda_k - \lambda^+.$$

III. FINITE DIFFERENCE APPROXIMATION OF THE MODEL EQUATION

3.1 Compact scheme and upwind compact scheme

Consider the model equation

$$\frac{\partial u}{\partial t} + \frac{\partial f}{\partial x} = 0, \quad f = Cu, \ C = \text{const}. \tag{5}$$

In Ref. 2, we gave the general expression for a two-layer scheme. A simple form is ($\alpha = 0$ and $\gamma = 0$)

$$(1+\frac{\beta}{2}\frac{\Delta t}{\Delta x}\delta_x C\cdot)\delta_t u_j^{n+1} = -\frac{\Delta t}{\Delta x}\delta_x C u_j^n, \tag{6}$$

$$u_j^{n+1} = u_j^n + \delta_t u_j^{n+1},$$

where $\beta \geqslant 1$ and δ_x is the differencing operator for spatial coordinates. Different methods of decomposition, different differencing operators for the spatial coordinates, as well as different values of β may be used in (6). If we take $\beta = 1$, Eq. (6) is an approximation with second-order accuracy. The accuracy in the spatial direction depends entirely on the actual form used for δ_x on the right-hand side. It is easy to see that if no odd characteristics are introduced in decomposing the coefficient C, the form of the decomposition cannot change the order of accuracy of the approximation scheme. For aerodynamic equations, it is necessary to overcome the discontinuity in the derivatives of $f^{\pm}$ with respect to u. For this reason, it is necessary to correct the decomposition methods of types (a) and (b) above. For type (c), it is easy to construct decomposed flow vectors $f^{\pm}$ with continuous derivatives in u.

One upwind compact difference approximation scheme for (5) is[3]

$$(1+\frac{\beta}{2}\frac{\Delta t}{\Delta x}\delta_x^- C^+ \cdot + \frac{\beta}{2}\frac{\Delta t}{\Delta x}\delta_x^+ C^- \cdot)\delta_t u_j^{n+1} = -\frac{\Delta t}{\Delta x}(F)_j^n , \tag{7}$$

$$F_j^{\pm} = \frac{\delta_x^0 - 2\varepsilon_4^{\pm}\delta_x^2}{1+2(\varepsilon_2^{\pm}-\varepsilon_4^{\pm})\delta_x^0 + (\frac{1}{6}-\varepsilon_3^{\pm})\delta_x^2} f_j^{\pm} , \quad F = F^+ + F^- , \tag{8}$$

where

$$C^+ + C^- = C , \quad C^+ \geqslant 0 , \quad C^- \leqslant 0 ,$$

$$\delta_x^+ g_j = g_{j+1} - g_j , \quad \delta_x^0 = \frac{1}{2}(\delta_x^+ + \delta_x^-) ,$$

$$\delta_x^- g_j = g_j - g_{j-1} , \quad \delta_x^2 = \delta^+\delta_x^- .$$

The expansion of (8) takes the form

$$\alpha_0^{\pm} F_{j+1}^{\pm} + \beta_0^{\pm} F_j^{\pm} + \gamma_0^{\pm} F_{j-1}^{\pm} = (a_0^{\pm}\delta_x^+ + b_0^{\pm}\delta_x^-) f_j^{\pm} , \tag{9}$$

$$\alpha_0^{\pm} = \frac{1}{6} + \varepsilon_2^{\pm} - \varepsilon_3^{\pm} - \varepsilon_4^{+} , \quad a_0^{\pm} = \frac{1}{2} - 2\varepsilon_4^{\pm} ,$$

$$\beta_0^{\pm} = \frac{2}{3} + 2\varepsilon_3^{\pm} , \qquad b_0^{\pm} = \frac{1}{2} + 2\varepsilon_4^{\pm} , \tag{10}$$

$$\gamma_0^{\pm} = \frac{1}{6} - \varepsilon_2^{\pm} - \varepsilon_3^{\pm} + \varepsilon_4^{\pm} .$$

If we make a Taylor series expansion of (9) at point j, we obtain

$$F_j^{\pm} = C\Delta x\frac{\partial u}{\partial x} - 2C\varepsilon_2^{\pm}\Delta x^2\frac{\partial^2 u}{\partial x^2} + C\varepsilon_3^{\pm}\Delta x^3\frac{\partial^3 u}{\partial x^3} + \varepsilon_4^{\pm}C\frac{\Delta x^4}{6}\frac{\partial^4 u}{\partial x^4} + \cdots . \tag{11}$$

It is easy to see that, when $C>0$, $\varepsilon_2^+ \geqslant 0$, and $\varepsilon_4^+ \geqslant 0$, the terms on the right-hand side of (7) produce a positive dissipation. When $C<0$, it is necessary to take ε_2^- and ε_4^- less than zero. From (11), we find also that, if we take

$$\varepsilon_k = O(\Delta x^{M+1-k}) , \quad M \leqslant 4 ,$$

the ratio $F_j/\Delta x$ approaches the derivative $\partial f/\partial x$ with order M.

Let us now give two very simple upwind compact difference schemes:

$$\text{(a)} \qquad \varepsilon_2^{\pm}=0\ ,\ \varepsilon_3^{+}+\varepsilon_4^{+}=\frac{1}{6}\ ,\ \varepsilon_3^{-}-\varepsilon_4^{-}=\frac{1}{6}\ , \tag{12}$$

$$\text{(b)} \qquad \varepsilon_2^{\pm}=\varepsilon_3^{\pm}=0,\ \varepsilon_4^{+}=\frac{1}{6}\ ,\ \varepsilon_4^{-}=-\frac{1}{6}\ , \tag{13}$$

In the first case, the accuracy of the approximation is $O(\Delta x^2)$. For the second case, it is $O(\Delta x^3)$. For these two cases, (9) may be written as

$$\beta_0^{+}F_j^{+}+\gamma_0^{+}F_{j-1}^{+}=(a_0^{+}\delta_x^{+}\cdot\ +b_0^{+}\delta_x^{-}\cdot\ )f_j^{+}\ , \tag{14}$$

$$\alpha_0^{-}F_{j+1}^{-}+\beta_0^{-}F_j^{-}\ =(a_0^{-}\delta_x^{+}\cdot\ +b_0^{-}\delta_x^{-}\cdot\ )f_j^{-}\ . \tag{15}$$

Equation (14) may be solved along the direction of increasing j, and (15) may be solved along the direction of decreasing j. It is worth noting the defining parameters of (14). Here, $F_j^{\pm}/\Delta x$ approaches $\partial f^{\pm}/\partial x$ with third-order accuracy. However, it is simpler than the usual third-order accuracy upwind difference scheme and the amount of computation is also smaller.

3.2 Upwind compact scheme with dispersion control

(*a*) "*Dissipation analogy*" *of the dispersion term*. For a long time, artificial viscosity was widely used to overcome the nonphysical fluctuations in the numerical solution. Such a nonphysical viscosity may come from the difference scheme itself. Alternatively, it may be put in artificially. To improve the discrimination in the numerical solution, an anti-diffusion method was suggested in Ref. 4. The TVD type of schemes developed these days also make use of such an anti-diffusion concept. It is well known that in the usual first-order accuracy difference scheme, such as the two-point upwind scheme, the numerical solution tends to be overly smooth in the vicinity of shock waves. Anti-diffusion methods try to control the diffusion so as to increase the accuracy and prevent fluctuations in the numerical solutions around shock waves. With anti-diffusion, the schemes remain to be dispersive. To improve the accuracy of the approximation, anti-diffusion often leads to third-order derivatives. Let us now examine the effect of the third-order derivative (i.e., dispersion) terms.

The corrected form of the usual second-order accuracy equation may be written in the form

$$\frac{\partial u}{\partial t}+\frac{\partial f}{\partial x}\cdot=\Delta x^2\frac{\partial}{\partial x}\left[\sigma\, C\,\frac{\partial^2 u}{\partial x^2}\right]+O(\Delta x^3)\ . \tag{16}$$

Here, C is taken to be a constant. Let us now examine the changes in the dispersion terms near shock waves. By shock wave we mean here a transition region in space. In such a small region, the variations in the flow parameters are very steep; however, continuous derivatives exist (see Fig. 1). Let the turning point ($\partial^2 u/\partial x^2=0$) of a curve be at S. For $C>0$, we shall call the right-hand side of point S the front of the wave and the left-hand side of S the back of the wave.

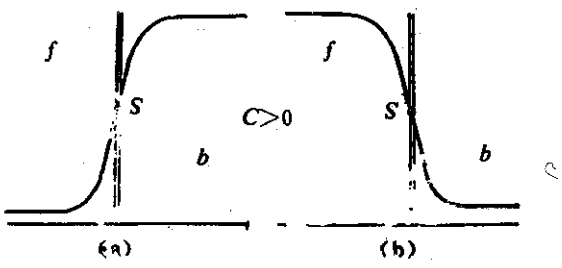

FIG. 1. Variations of u at time t.

The front of the wave will be represented by f and the back by b. Near a shock wave, $\partial u/\partial x \neq 0$ and it is possible to rewrite (16) as

$$\frac{\partial u}{\partial t} + \frac{\partial f}{\partial x} = \frac{\partial}{\partial x} k \frac{\partial u}{\partial x}, \tag{17}$$

where

$$k = \Delta x^2 \sigma C \frac{\partial^2 u}{\partial x^2} \Big/ \frac{\partial u}{\partial x}. \tag{18}$$

Naturally, we require that $k \geqslant 0$, otherwise the corresponding problem may not be well defined. Let $\sigma C > 0$ (a similar discussion can also be carried out for $\sigma C < 0$). Behind the wave, we have $\partial U/\partial x > 0$ and $\partial^2 U/\partial x^2 > 0$, as shown in Fig. 1(a). In front of the wave we have $\partial U/\partial x < 0$ and $\partial^2 U/\partial x^2 < 0$, as shown in Fig. 1(b). As a result, $k > 0$ behind the wave, $k = 0$ at S, and $k < 0$ in front of the wave. Since the dissipation-analogy coefficient in front of the wave is negative, the condition $k \geqslant 0$ is not satisfied. This is why fluctuations in the numerical solution occur in ordinary second-order accuracy difference schemes. We can take the right-hand side of (17) as the artificial viscosity to correct (5) and take $\sigma C > 0$. If we further restrict the coefficient k to take on the form of (18) such that $k \geqslant 0$ both in front and behind the wave, we can expect improvement in the behavior of the numerical solution near shock waves. The upwind compact scheme with dispersion control, which we shall introduce later, is constructed based on such considerations. In Ref. 5, the requirements on the coefficients of third-order derivatives are discussed in terms of the method of small-perturbation analysis.

(*b*) *Dispersion errors in the* TVD *scheme.* In order to increase the ability to capture shock waves, different types of TVD schemes have been developed. By controlling the amount of anti-diffusion, the total changes in the differences in the solutions are made to decrease or have limitations put on them. We shall make use of the dispersion analogy idea mentioned earlier to construct a partial TVD-like scheme. We may consider that different TVD schemes are different by the use of different methods to control the dissipation analogy coefficient k. In these methods, the minmod function is often used to carry out the control. Let us now carry out a simple analysis of a TVD type of scheme[6] that is close to (5). The approximate equation may be written as

$$\frac{\partial u}{\partial t} + \frac{1}{\Delta x}\left[\tilde{h}_{j+\frac{1}{2}} - \tilde{h}_{j-\frac{1}{2}}\right] = 0, \tag{19}$$

$$\tilde{h}_{j+\frac{1}{2}} = \frac{1}{2}\left[\tilde{f}_j + \tilde{f}_{j+1} - \psi(\tilde{c}_{j+\frac{1}{2}})\delta_{j+\frac{1}{2}} u\right],$$

$$\tilde{f}_j = f_j + g_j,$$

$$g_j = \mathrm{minmod}\{\sigma_{j+\frac{1}{2}}\delta_{j+\frac{1}{2}} u, \sigma_{j-\frac{1}{2}}\delta_{j-\frac{1}{2}} u\}, \tag{20}$$

$$\delta_{j+\frac{1}{2}} u = u_{j+\frac{1}{2}} - u_j,$$

$$\mathrm{minmod}\{x, y\} = \mathrm{sign}(x)\cdot \max\{0, \min[|x|, y\,\mathrm{sign}(x)]\}, \tag{21}$$

$$\tilde{c}_{j+\frac{1}{2}} = C^+_{j+\frac{1}{2}} + \gamma_{j+\frac{1}{2}},$$

$$\gamma_{j+\frac{1}{2}} = \begin{cases} \dfrac{g_{j+1} - g_j}{\delta_{j+\frac{1}{2}} u} & \text{when } \delta_{j+\frac{1}{2}} u \neq 0 \\ 0 & \text{when } \delta_{j+\frac{1}{2}} u = 0. \end{cases}$$

When $C =$ constant, we have

$$C_{j+\frac{1}{2}} = C,\ \psi(z) = |z|,\ \sigma_{j+\frac{1}{2}} = \frac{1}{2}\psi(C),$$

$$g_{j+\frac{1}{2}} = \sigma\ \text{minmod}\{\delta_{j+\frac{1}{2}}u\ ,\ \delta_{j-\frac{1}{2}}u\ \}.$$

By making a Taylor series expansion we obtain the corrections corresponding to (19)

$$b:\ \frac{\partial u}{\partial t} + \frac{\partial f}{\partial x} = \frac{C}{3}\Delta x^2 \frac{\partial^3 u}{\partial x^3} + \cdots, \tag{22a}$$

$$f:\ \frac{\partial u}{\partial t} + \frac{\partial f}{\partial x} = -\frac{C}{6}\Delta x^2 \frac{\partial^3 u}{\partial x^3} + \cdots. \tag{22b}$$

If we rewrite (22) in the same form as (17), the dissipation analogy coefficient corresponding to third-order derivatives are positive both before and after the wave. Many of the available TVD schemes may be obtained using such a dissipation analogy method. Since the denominator of the analogy coefficient k contains first-order derivatives, the accuracy of the approximation decreases in order at the extrema.

(*c*) *Upwind compact finite difference with dispersion control.* There are three free parameters in the upwind compact scheme and they may be used to control the accuracy of the approximation in the spatial direction, or the dissipation characteristics of the scheme and the dispersion accuracy. To make the scheme diffusive, it is necessary that $\varepsilon_{2,4}^{+} > 0$ and $\varepsilon_{2,4}^{-} < 0$. To construct the third-order derivative terms in (11) (those containing $\varepsilon_3^{\pm}$) the corresponding dissipation-analogy coefficient k must be positive. Control over the dispersion term is exercised through parameters $\varepsilon_3^{\pm}$. In practice, when $C > 0$, it is necessary that $\varepsilon_3^{+} < 0$ behind the shock wave and $\varepsilon_3^{+} > 0$ in front. It is possible to use the dispersion adjustment coefficient introduced below to make $\varepsilon_3^{\pm}$ change its own sign in going through a shock wave.

IV. COMPACT SCHEME FOR AERODYNAMIC EQUATIONS WITH DISSIPATION CONTROL

In the upwind compact scheme with dispersion control, the approximation for a one-dimensional Euler equation is

$$(I + \frac{\beta}{2}\frac{\Delta t}{\Delta x}\delta_x^{-}A^{+}\cdot + \frac{\beta}{2}\frac{\Delta t}{\Delta x}\delta_x^{+}A^{-}\cdot)\delta_t U_j^{n+1} = -\frac{\Delta t}{\Delta x}F_j^n, \tag{23}$$

$$U^{n+1} = U^n + \delta_t U^{n+1},$$

$$F_j = F_j^{+} + F_j^{-},$$

$$F_j^{\pm} = \frac{\delta_x^0 - 2\varepsilon_4^{\pm}\delta_x^2}{1 + 2(\varepsilon_2^{\pm} - \varepsilon_4^{\pm})\delta_x^0 + (\frac{1}{6} - \varepsilon_3^{\pm})\delta_x^2} f_j^{\pm}. \tag{24}$$

Here I is the unit matrix, $A^{\pm}$ and $f^{\pm}$ are the Jacobian coefficient matrix and the flow vector after the decomposition, respectively. When we take $\beta = 1$, (23) has second-order accuracy in time. The accuracy in the spatial direction is determined by the choice of the parameter $\varepsilon_k^{\pm}$. In the calculations carried out in this work, we have taken $\varepsilon_2^{\pm} = 0$ and $\varepsilon_4^{\pm} = \pm 0.125$.

We shall now give an expression for $\varepsilon_3^{\pm}$. Let the dispersion matching coefficient be

$$G(e_j) = -\varepsilon_0 \frac{|e_{j+1} - e_j| - |e_j - e_{j-1}|}{|e_{j+1} - e_j| + |e_j - e_{j-1}|},\quad e = \rho, p. \tag{25}$$

Here ε^0 is a free positive parameter. The matching coefficient $G(e_j)$ is positive in front of the wave and negative behind the wave. In the smooth regions, $G \approx \Delta x$. For the calculations in this work, we have taken

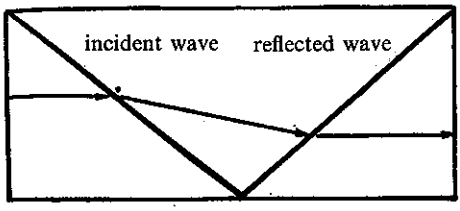

FIG. 2. Schematic diagram showing the reflection of shock waves.

$$\varepsilon_3^{\pm} = \pm G(e_j)\,. \tag{26}$$

By taking the parameter $\varepsilon_k^{\pm}$ in the way mentioned above, the scheme has third-order accuracy without having the problem of having lower orders of accuracies at extrema. The scheme is dissipative and the coefficient for the dispersion terms in front and behind the wave is adjusted automatically according to the need. In this way, the dissipation analogy coefficient is always non-negative near a shock wave.

Equation (23) may be solved directly. Here we have to find the inverse of a block tri-diagonal matrix. It is also possible to find the solution for the implicit part using approximate coefficient decomposition. We shall adopt the latter method to carry out the calculations here. For the matrices after the decomposition, we shall use the second type of decomposition method mentioned in Sec. II.

There are two types of method to decompose $f^{\pm}$ in (24). The first is the third method suggested by the present authors. It has been pointed out earlier that different methods of decomposition cannot affect the order of accuracy—only the coefficients of the cutoff error.

V. NUMERICAL EXPERIMENTS

We have carried out calculations for a two-dimensional Euler equation for the shock-wave reflection problem using methods described above. The schematic diagram for the flow is shown in Fig. 2. The incoming flow Mach number is $M_\infty = 2.9$, the incident angle for the shock wave is 29°, and the region covered by the calculation is $0 \leqslant x \leqslant 4$ and $0 \leqslant y \leqslant 1$. The number of points in the mesh is $\mathrm{IN}(x) \cdot \mathrm{JN}(y) = 81 \times 41$. The results shown in Fig. 3 are obtained with a two-point upwind scheme. The first method of decomposition in Sec. II is used in the calculations. From the figure we can see a serious problem in having the shock waves be smoothed out.

The results given in Fig. 4 are obtained with $\varepsilon_k^{\pm} = \text{constant}$, i.e., $\varepsilon_2^{\pm} = \varepsilon_3^{\pm} = 0$ and $\varepsilon_4^{\pm} = \pm 1/6$. Only the dissipation characteristics of the scheme are used here and no dispersion control is applied. From the figure we see that the numerical solution is improved near the

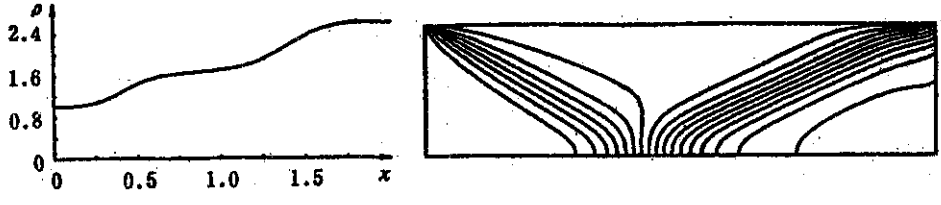

FIG. 3.(a) Density distribution (two-point upstream scheme with $J = 21$). (b) Lines of equal density (two-point upstream scheme).

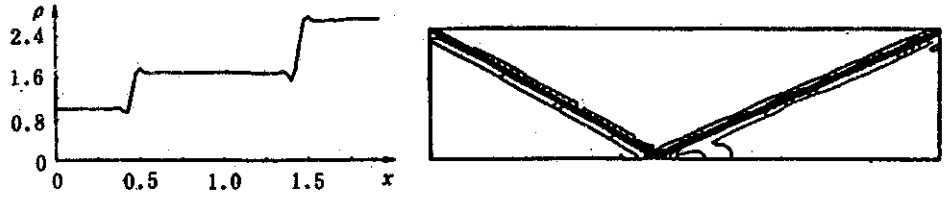

FIG. 4.(a) Density distribution ($\varepsilon_2^{\pm}=0,\varepsilon_3^{\pm}=0,\varepsilon_4^{\pm}=\pm\frac{1}{6},J=21$). (b) Lines of equal density ($\varepsilon_2^{\pm}=0,\varepsilon_3^{\pm}=0,\varepsilon_4^{\pm}=\pm\frac{1}{6}$).

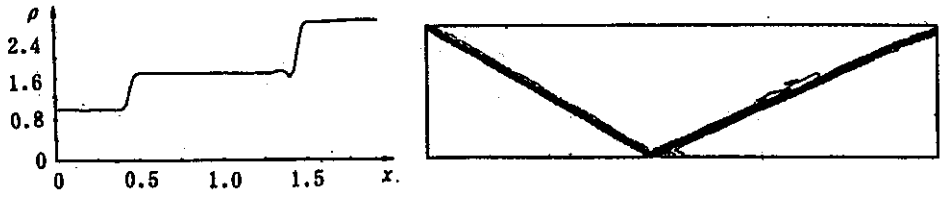

FIG. 5.(a) Density distribution (type a decomposition $\varepsilon_2^{\pm}=0$, $\varepsilon_3^{\pm}\approx G(p_j)$, $\varepsilon_4^{\pm}=\pm 0.125$, $J=21$). (b) Lines of equal density (type a decomposition $\varepsilon_2^{\pm}=0$, $\varepsilon_3^{\pm}\approx G(p_j)$, $\varepsilon_4^{\pm}=\pm 0.125$).

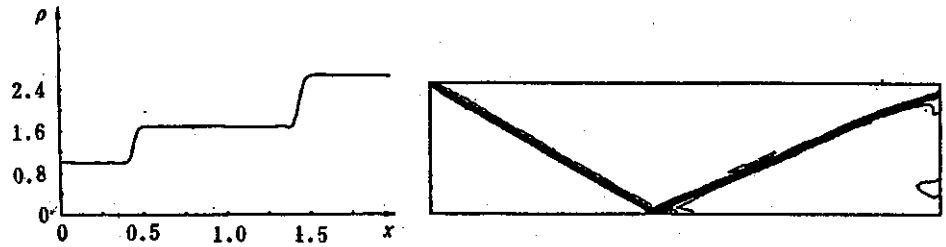

FIG. 6.(a) Density distribution (type a decomposition $\varepsilon_2^{\pm}=0$, $\varepsilon_3^{\pm}\approx G(\rho_j)$, $\varepsilon_4^{\pm}=\pm 0.125$, $J=21$). (b) Lines of equal density (type a decomposition $\varepsilon_2^{\pm}=0$, $\varepsilon_3^{\pm}\approx G(\rho_j)$, $\varepsilon_4^{\pm}=\pm 0.125$).

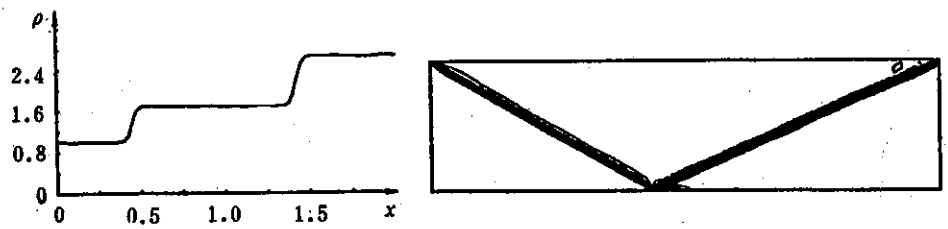

FIG. 7.(a) Density distribution (type c decomposition $\varepsilon_2^{\pm}=0$, $\varepsilon_3^{\pm}\approx G(\rho_j)$, $\varepsilon_4^{\pm}=\pm 0.125$, $J=21$). (b) Lines of equal density (type c decomposition $\varepsilon_2^{\pm}=0$, $\varepsilon_3^{\pm}\approx G(\rho_j)$, $\varepsilon_4^{\pm}=\pm 0.125$).

shock wave, with only small fluctuations present.

The results in Figs. 5 to 7 are obtained with dispersion control using $\varepsilon_2^{\pm} = 0$ and $\varepsilon_4^{\pm} = \pm 0.125$. The first type of decomposition given in Sec. II is used in obtaining the results shown in Fig. 5 and we take $e_j = p_j$ in (25). We can see from the figure that there are only small fluctuations in front of the reflected wave. As a whole, the results are satisfactory. The results shown in Fig. 6 are obtained using the first type of decomposition with $G(e_j) = G(\rho_j)$. The results shown in Fig. 7 are obtained using the third type of decomposition.

VI. CONCLUSION

We have developed here an upwind compact scheme with control over dispersion errors. The method is simple and the amount of computation required is small. It also has the advantage of high accuracy and captures shock waves effectively. In smooth regions, it has consistently high degrees of accuracy. We have used a third-order accuracy upwind compact scheme with dispersion control to evaluate a two-dimensional shock wave reflection problem and the results are very satisfactory.

*Supported by the National Natural Science Foundation of China

[1] Ma Yanwen, *High precision finite difference scheme for purely supersonic, dissipative, viscous circular flow problem*, Conf. on Computational Aerodynamics (1978).

[2] Ma Yanwen and Fu Dexun, AIAA No. 87-1123.

[3] Fu Dexun and Ma Yanwen, in *Collection of Works on International Symposium on Computational Fluid Dynamics*, Nagoya (1989).

[4] J. P. Boris and D. L. Book, J. Comp. Phys. **11**, 38 (1973).

[5] Zhang Hanxin, *Kong Qi Dong Li Xue Xue Bao* (Aerodynamics in Chinese) **1**, (1984).

[6] H. C. Yee, R. F. Warming, and A. Harten, J. Comp. Phys. **57**, 3 (1985).

Translated by S. S. M. Wong
Edited by G. M. Temmer